

3  
4 **Subantarctic Mode Water Biogeochemical Formation Properties and Interannual**  
5 **Variability**

6  
7 Seth M. Bushinsky<sup>1</sup> and Ivana Cerovečki<sup>2</sup>

8  
9 <sup>1</sup>Department of Oceanography, School of Ocean and Earth Science and Technology, University  
10 of Hawai‘i at Mānoa, Honolulu, HI

11 <sup>2</sup>Scripps Institution of Oceanography, University of California San Diego, La Jolla, CA  
12

13 **Contents of this file**

14 Text S1 to S4

15 Figures S1 to 5

16 Table S1  
17

18 **Introduction**

19 Included in the Supporting Information are figures to supplement those in the main text  
20 and a table that indicates float observations identified as bad.  
21

22 **Text S1. Float biogeochemical observations**

23 Only float data flagged as “good” were used for this analysis. Observations in the upper 20  
24 m for each float were assessed to identify large anomalous changes in individual biogeochemical  
25 tracers that do not correspond to observed changes in temperature, salinity, or other  
26 biogeochemical parameters. Obvious outliers were removed from the analysis dataset (Table S1).  
27 Note that these are profiles removed from the entire float dataset prior to filtering for data that fall  
28 in the relevant SAMW formation areas. Most of the removed data therefore do not impact this  
29 study but are included to allow reproducibility of the original dataset considered.

30 The relationship between density and wintertime mixed layer properties is similar between  
31 the Pacific and Indian Oceans (Fig S1). This indicates that the differences in mean properties

32 between SAMW that forms in each region are due to the different densities of the waters that form  
33 in these regions.

34 Differences between Biogeochemical Southern Ocean State Estimate (BSOSE) properties  
35 output sampled at float locations and actual float measurements or derived quantities are shown in  
36 Fig. S2. Differences are shown for the upper 200 m, using data from August and September float  
37 profiles when float calculated MLD is at least 200 m. Averages from the upper 200 m only were  
38 used to avoid the impact of differing BSOSE and float MLDs on the comparisons as profile  
39 differences are at a maximum at the high tracer gradients just below the MLD.

40

#### 41 **Text S2. Calculation of $\Delta p\text{CO}_2$**

42  $\Delta p\text{CO}_2$  ( $\mu\text{atm}$ ) values were calculated using the atmospheric  $\text{CO}_2$  mole fraction ( $x\text{CO}_2$   
43 ( $\mu\text{mol/mol}$ ), NOAA Greenhouse Gas Marine Boundary Layer Reference; Dlugokencky et al.  
44 2019) matched to the nearest latitude:

45

$$46 \quad p\text{CO}_{2,\text{atm}} = x\text{CO}_2 \left( \frac{\text{SLP}}{1013.25} - p\text{H}_2\text{O} \right) \quad (1)$$

$$47 \quad \Delta p\text{CO}_2 = p\text{CO}_{2,\text{surf}} - p\text{CO}_{2,\text{atm}} \quad (2)$$

48

49 where  $p\text{CO}_{2,\text{surf}}$  is the seawater  $p\text{CO}_2$ ,  $p\text{CO}_{2,\text{atm}}$  is the atmospheric partial pressure of  $\text{CO}_2$  adjusted  
50 for local climatological sea level pressure (SLP, (mbar)) and water vapor pressure ( $p\text{H}_2\text{O}$  (atm),  
51 calculated from sea surface temperature (SST) and sea surface salinity (SSS); Zeebe and Wolf-  
52 Gladrow 2001). The average  $p\text{H}_2\text{O}$  for the wintertime float data used in this study was 0.01 atm  
53 ( $\sim 4 \mu\text{atm}$  impact on  $p\text{CO}_2$ ).

54 In order to compare  $\Delta p\text{CO}_2$  between different years we calculated a 10-year climatology  
55 of sea level pressure from National Centers for Environmental Prediction (NCEP; Kalnay et al.,  
56 1996) reanalysis sea level pressure at the location of each observation. We fit a seasonal harmonic  
57 to the 2011 to 2020 SLP and used each observation's day of year to determine SLP for the  $\Delta p\text{CO}_2$   
58 calculation (equations 1 and 2). We used this approach to avoid the impact of short-term variations  
59 in pressure, such as storms, that might not be equally distributed between float and shipboard  
60 datasets. The mean  $\pm 1$  SD correction to SLP was  $-0.7 \pm 13.9$  mbar (in situ SLP minus  
61 climatological SLP), which equated to a  $\Delta p\text{CO}_2$  correction of  $-0.8 \pm 5.3 \mu\text{atm}$  ( $\Delta p\text{CO}_2$  calculated

62 using in situ SLP minus  $\Delta p\text{CO}_2$  using climatological SLP). While the average correction is small,  
63 this ensures that there are no large differences in  $\Delta p\text{CO}_2$  due to short-term pressure variations.

64

### 65 **Text S3. Crossover comparison between SOCAT and float $p\text{CO}_2$ .**

66 Prior studies comparing shipboard  $p\text{CO}_2$  from the SOCAT dataset and float pH-derived  
67  $p\text{CO}_2$  found that SOCCOM float  $p\text{CO}_2$  estimates might be high by approximately 4  $\mu\text{atm}$   
68 (Williams et al. 2017; Fay et al. 2018; Gray et al. 2018). Here we perform an updated crossover  
69 comparison between the May 2021 SOCCOM snapshot and the Surface Ocean  $\text{CO}_2$  Atlas v2021  
70 (SOCAT; Bakker et al. (2016)). Crossovers were determined by finding float profiles and SOCAT  
71 measurements within  $\pm 1$  day and  $\pm 25$  km ( $n=87$ ). Only crossover comparisons with a density  
72 difference less than  $0.03 \text{ kg m}^{-3}$  were used for this analysis (Fig. S3,  $n=52$ ).  $p\text{CO}_2$  values were  
73 recalculated using CO2SYS (van Heuven et al. 2011) to account for any temperature difference  
74 between matched observations. The mean difference between SOCAT and SOCCOM  $p\text{CO}_2$   
75 was  $-1.86 \pm 15.8 \mu\text{atm}$  (SOCAT minus SOCCOM).

76

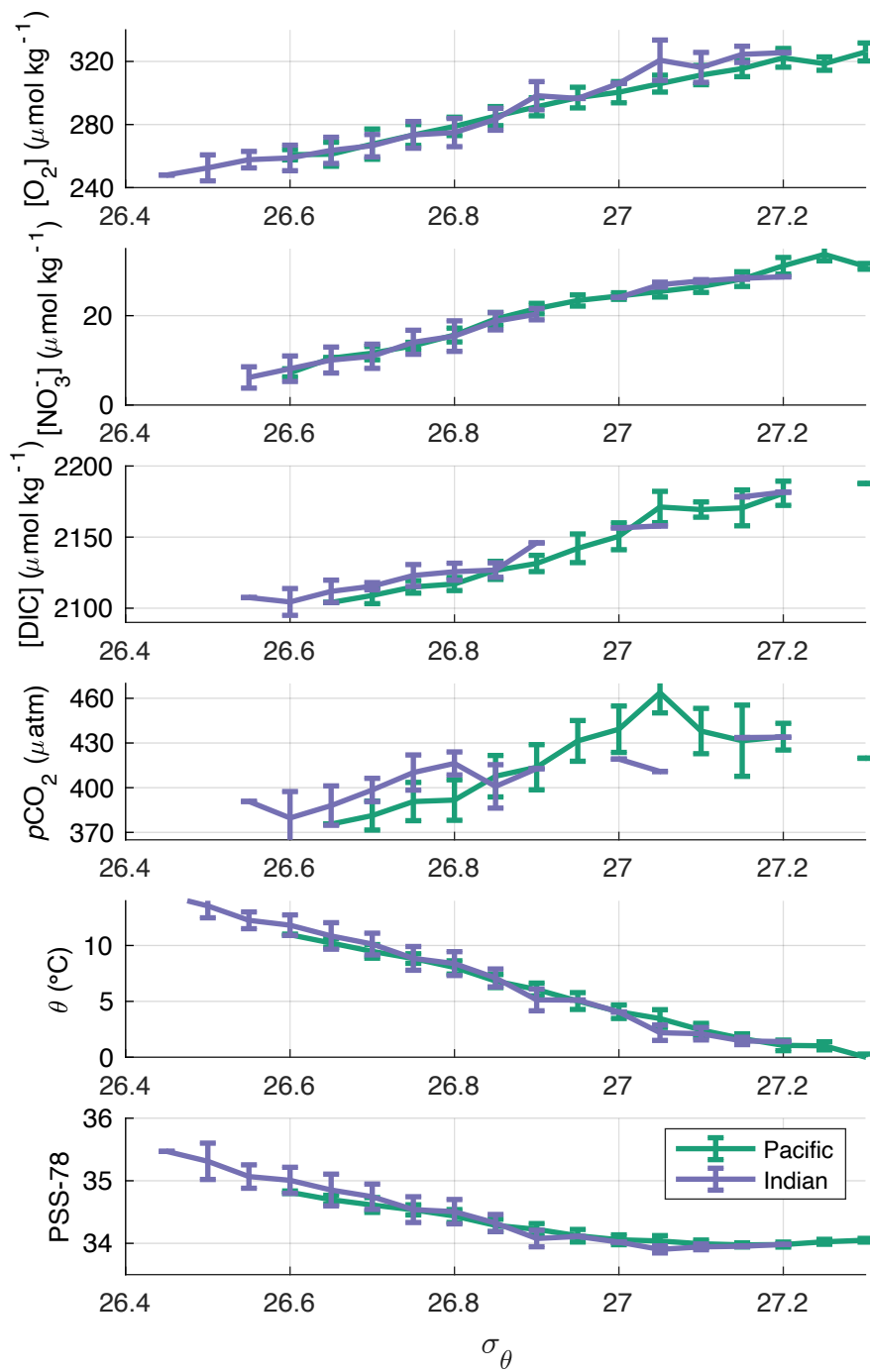
### 77 **Text S4. Biogeochemical Southern Ocean State Estimate**

78 Interannual variability of biogeochemical properties in the Pacific and central and southeast  
79 Pacific sub-regions was assessed using BSOSE. BSOSE mean winter (August and September) ML  
80 oxygen concentrations of SAMW formation areas in all regions maintained a fairly consistent  
81 negative (undersaturated)  $\Delta[\text{O}_2]$  of  $\sim 11 \mu\text{mol kg}^{-1}$  with an  $[\text{O}_2]$  range of 285-301  $\mu\text{mol kg}^{-1}$  (Fig.  
82 S4). Comparable annual averages from float observations display a similar  $\Delta[\text{O}_2]$ , though with a  
83 lower range in  $[\text{O}_2]$  of 273-295  $\mu\text{mol kg}^{-1}$ .  $[\text{O}_2]_{\text{saturation}}$  as a function of temperature (constant  
84  $S=34.2$ ) is plotted with no correction for sea level pressure (black dashed line) and with a  
85 correction for mean winter SLP at the float profile locations (gray dot-dashed line, calculated from  
86 NCEP pressure reanalysis as described in Text S2).

87 BSOSE Pacific biogeochemical averages were determined from 3-D fields at locations  
88 where August or September MLD estimates are deeper than 150 m. This threshold was chosen to  
89 exclude shallower mixed layers that are not associated with SAMW formation, but at the same  
90 time to ensure we consider a continuous band of deep wintertime mixed layers. Anomalies of  
91 meridional averages reveal west to east propagation (Fig. S5). Together with local forcing, this

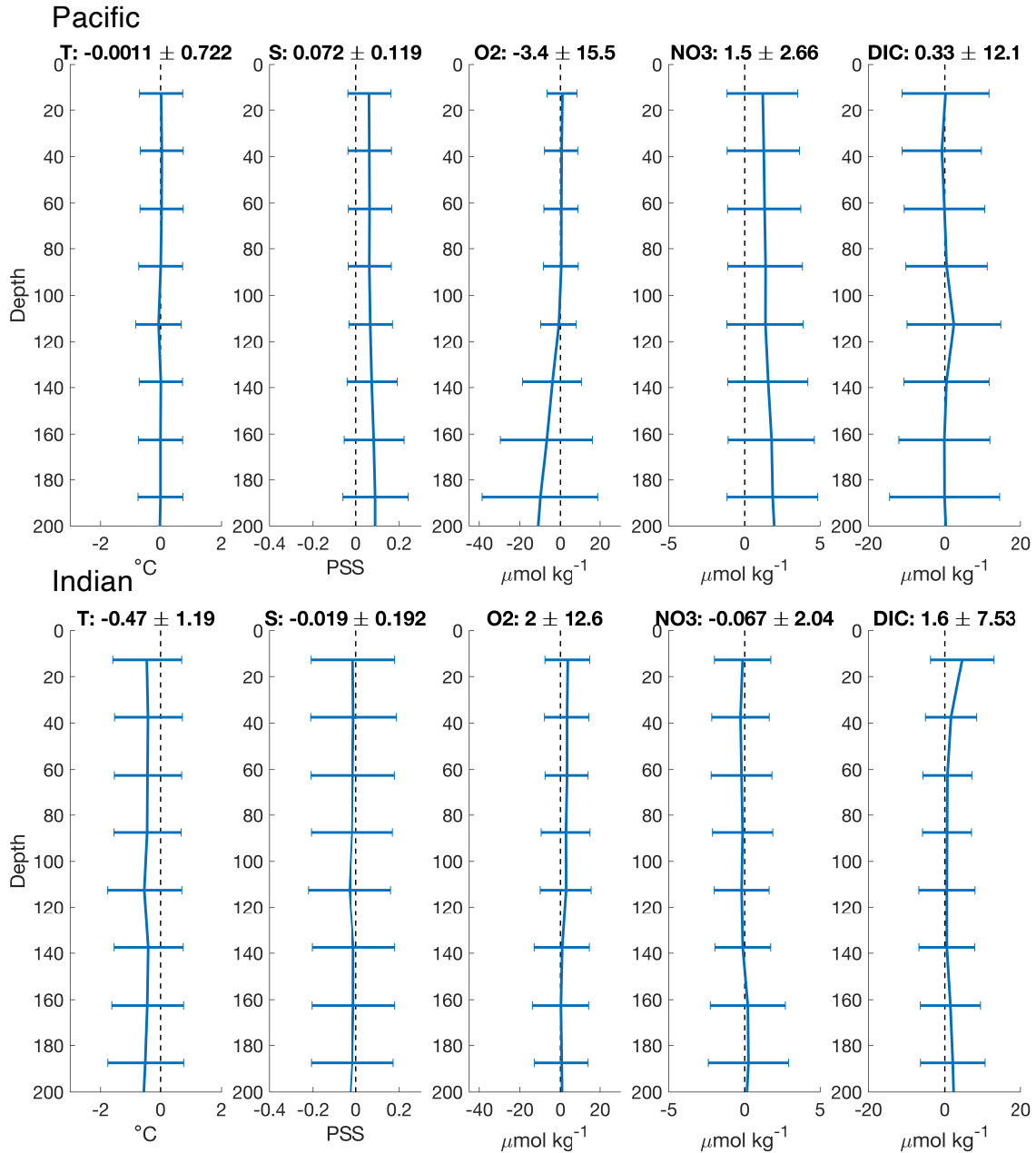
92 advective signal plays an important role in governing both overall Pacific and east-west differences  
93 in interannual variability.

94

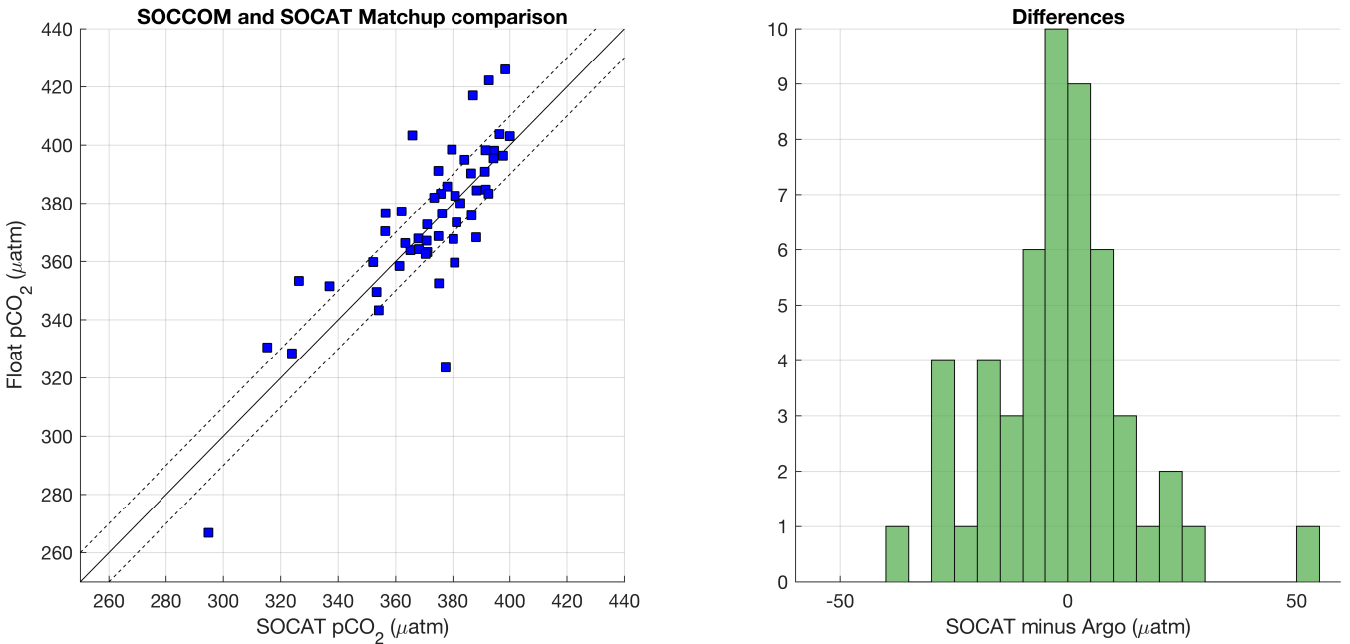


95  
 96 **Figure S1. Overlaid wintertime property vs. density relationships for the Pacific and Indian**  
 97 **Ocean sectors.** Properties are August and September mixed layer averages, gridded by density.  
 98 Only mixed layers deeper than 200 m are included.

99  
 100



101  
 102 **Figure S2. Mean differences between BSOSE output sampled at float locations and float**  
 103 **observations of temperature (T), salinity (S), oxygen (O<sub>2</sub>), nitrate (NO<sub>3</sub>), and dissolved**  
 104 **inorganic carbon (DIC).** Differences shown are BSOSE minus float, averaged in 25m depth bins  
 105 with error bars indicating RMSE for each bin. Panel titles contain average mean ± average RMSE  
 106 for upper 200 m. Data are only shown for August and September profiles when calculated MLD  
 107 is at least 200 m using the same geographic criteria as described in Section 2. BSOSE comparison  
 108 data are available at: <http://sose.ucsd.edu/SO6/ITER135/PROF/>.



110

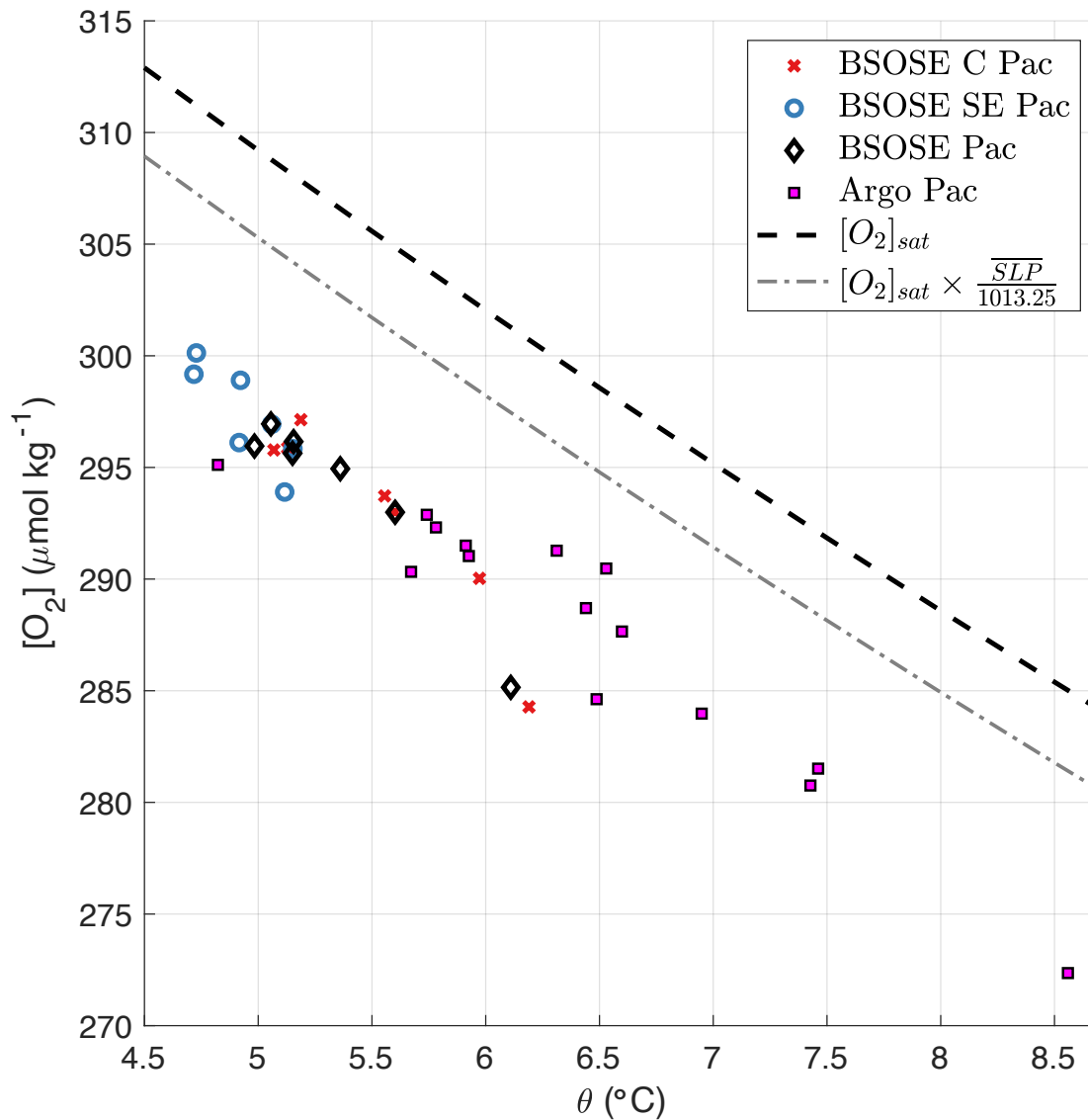
111 **Figure S3. Crossover comparison of float and SOCAT  $p\text{CO}_2$ .** Float and ship crossovers are  
 112 identified by finding observations within  $\pm 1$  day and  $\pm 25$  km. Float  $p\text{CO}_2$  estimates are averages  
 113 of data shallower than 10 db. SOCAT  $p\text{CO}_2$  data are the mean of all measurements within the  
 114 search criteria. Crossovers with a density different greater than  $0.03 \text{ kg m}^{-3}$  were removed (original  
 115  $n=87$ ,  $n=52$  after density filtering, left, blue squares). Solid black line is 1:1 line, dashed lines are  
 116  $\pm 10 \text{ } \mu\text{atm}$ . Mean SOCAT – Argo  $p\text{CO}_2$  is  $-1.86 \pm 15.8 \text{ } \mu\text{atm}$  (right).

117

118

119

120



121

122

123 **Figure S4. Winter oxygen concentration vs. potential temperature for Pacific and Pacific**

124 **sub-region core formation properties.** Yearly BSOSE winter (August and September) mixed

125 layer average oxygen concentrations from the central, southeast, and overall Pacific from the

126 available 2013-2019 output (red “x”, blue “o”, and black diamond symbols, respectively).

127 Black dashed line is solubility calculated from temperature with a fixed salinity of 34.2 and gray dot-

128 dashed line is the solubility corrected for mean SLP in the wintertime Pacific SAMW formation

129 regions. Magenta squares are averages of float observations for the overall Pacific.



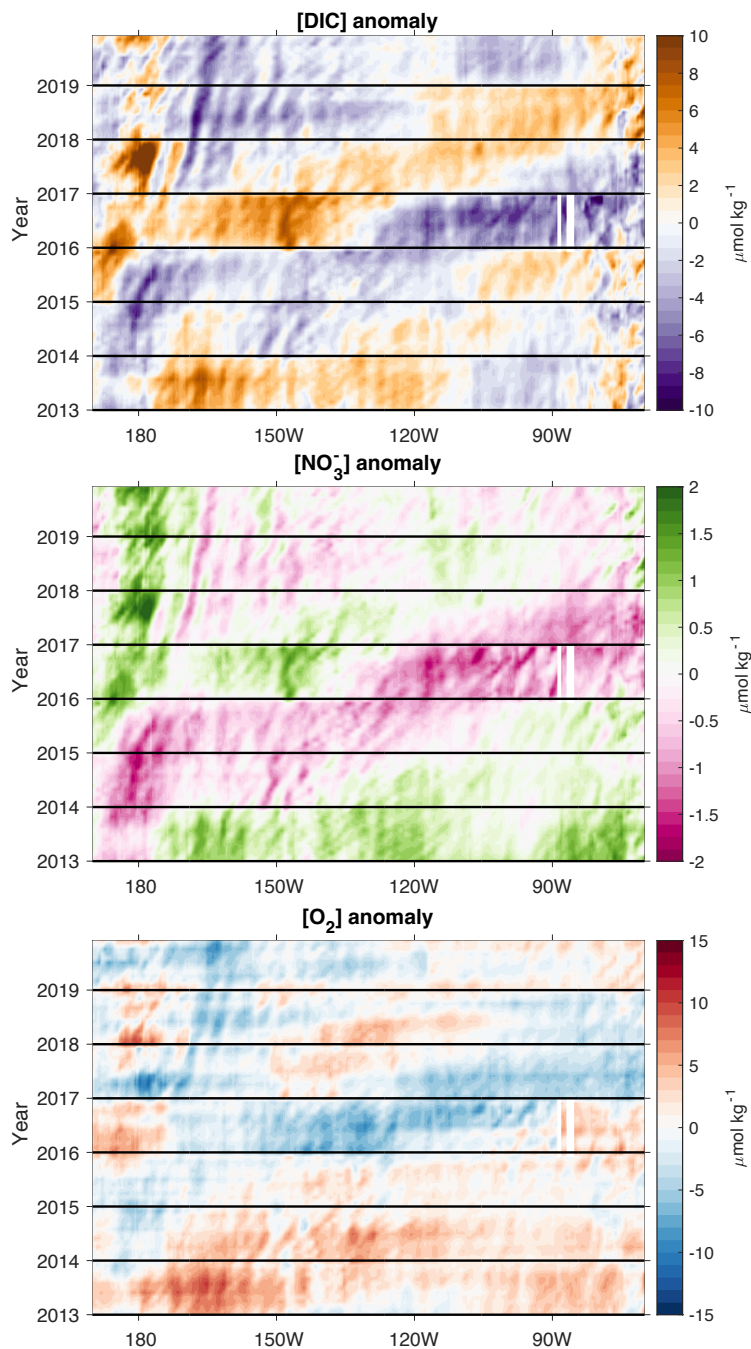


**Figure S5. Hovmöller diagrams of BSOSE Pacific [DIC], [NO<sub>3</sub><sup>-</sup>], and [O<sub>2</sub>] anomalies.** Meridional averages were constructed from 3-D fields masked using August-September MLDs when MLs were deeper than 150 m. The slightly shallower ML threshold (relative to the 200 m threshold used for determination of preformed SAMW properties) allowed consideration of a circumpolar band in order to follow the propagating signal. A 200 m. threshold shows a similar pattern but with more data gaps.

134 **Table S1**

Float UW SN	WMO #	Profile (sample number) <sup>1</sup>	Parameters affected
3900345	5027	162 - end	O <sub>2</sub> , Salinity
5901043	5020	109	O <sub>2</sub>
5901046	2342	177	O <sub>2</sub> , Salinity
5901047	5004	41	O <sub>2</sub>
5901049	2343	70	O <sub>2</sub>
5901051	2344	63 - 65	O <sub>2</sub>
5901310	5085	119 - end	O <sub>2</sub> , Salinity
5901313	5086	182	O <sub>2</sub>
5901736	5302	94 - end	O <sub>2</sub> , Salinity
5902100	5333	48 - end	O <sub>2</sub> , Salinity
5903382	6643	53 - end	O <sub>2</sub>
5904179	6091	125	O <sub>2</sub>
5904184	9091	122(3)	pH and derived vars.
5904657	9662	56, 82	pH and derived vars.
5904660	9652	38	pH and derived vars.
5904679	9757	83, 102	pH and derived vars., Salinity
5904686	510	101	pH and derived vars.
5904761	9660	16, 17, 20, 28, 56, 59	pH and derived vars.
5904844	9766	21	pH and derived vars.
5904984	569	34	O <sub>2</sub>
5905070	12537	109	O <sub>2</sub>
5906221	18796	25	O <sub>2</sub>

135 <sup>1</sup> Sample number is the float sample relative to the value nearest the surface (1). If no sample  
136 number is listed, the entire profile was set to NaN values.

137